Journal of Biological Physics **26:** 203–218, 2000.

Role of Mg^{2+} in Chromomycin A_3 – DNA Interaction: A Molecular Modeling Study

SUKANYA CHAKRABARTI[1], DIPAK DASGUPTA[2] and DHANANJAY BHATTACHARYYA[2*]

[1]*Chemistry Department, Lady Brabourne College, P1/2 Suhrawardy Avenue, Calcutta-700 017, India*

[2]*Biophysics Division, Saha Institute of Nuclear Physics, 37, Belgachia Road, Calcutta-700 037, India*

[*]*Author for correspondence, e-mail: bhatta@biop.saha.ernet.in*

Abstract. Chromomycin A_3 (CHR) is an antitumor antibiotic that inhibits macromolecular biosynthesis by reversibly binding to double stranded DNA *via* the minor groove, with GC-base specificity. At and above physiological pH when CHR is anionic, interaction of CHR with DNA requires the presence of divalent metal ions like Mg^{2+}. However, at acidic pH the molecule is neutral and it binds DNA even in absence of Mg^{2+}. Molecular dynamics simulation studies at 300K of neutral CHR and 1:1 CHR:Mg^{2+} complexes formed at pH 5.2 and 8.0 show that hydrophobicity of CHR:Mg^{2+} complex formed with the neutral drug is greater than that of the two other species. Interactions of CHR with DNA in presence and absence of Mg^{2+} have been studied by simulated annealing to understand the role of Mg^{2+} in the DNA binding potential of CHR. This shows that the antibiotic has the structural potential to bind to DNA even in the absence of metal ion. Evaluation of the direct interaction energy between the ligand and DNA does not explain the observed GC-base specificity of the antibiotic. When energy contributions from structural alteration of the interacting ligand and DNA as a sequel to complex formation are taken into account, a true picture of the theoretical binding propensity emerges. This implies that DNA and/or the ligand undergo significant structural alterations during the process of association, particularly in presence of Mg^{2+}. Accessible surface area calculations give idea about the entropy contribution to the binding free energy which is found to be different depending upon the presence and absence of Mg^{2+}.

Key words: Accessible surface area, antitumor antibiotic, GC-base specificity, Hydrophobicity, MD simulation, simulated annealing

1. Introduction

Chromomycin A_3 (CHR, Figure 1) and structurally related mithramycin (MTR) are two antitumor antibiotics of the aureolic acid group. These antibiotics bind non-covalently to the minor groove of double stranded DNA in the presence of divalent metal ions like Mg^{2+} with GC-base specificity and inhibits macromolecular biosynthesis *in vivo* [1]. Biophysical studies have indicated that hydrogen bonding between 2-amino group of guanine residues and oxygens of the chromophore in

antibiotic leads to GC base specific recognition [2–4]. Structurally both antibiotics contain the same chromophore but differ in the nature of the sugar residus connected on either sides of the aureolic acid group. At and above physiological pH, both the drugs are negatively charged (hydroxyl group at the C9 of the chromophore is deprotonated) with different pK_a values (7.0 and 5.0 for CHR and MTR, respectively, [5]). Thus, Mg^{2+} requirement during the drug-DNA association was ascribed to minimizing the forces of repulsion between the negatively charged phosphodiester backbone of DNA and the antibiotic. Subsequent studies, however did not support the idea that the metal ion is necessary as a mere counterion [5, 6]. However these studies could not assign the role of Mg^{2+} at the molecular level. Two questions, relevant for understanding the structural basis of drug-DNA interaction in the presence of Mg^{2+}, are (i) assessment of the structural potential of the antibiotic to bind DNA in the absence of Mg^{2+} and (ii) the role of Mg^{2+} in the association process. It was shown for the first time from our laboratory that these anionic antibiotics (at pH 8.0) form two types of complexes with Mg^{2+}, even in the absence of DNA namely, (drug):Mg^{2+} [complex I] with 1:1 stoichiometry and $(drug)_2$:Mg^{2+} [complex II] with 2:1 stoichiometry [6, 7]. These complexes are the DNA binding ligands at and above neutral pH. NMR studies also indicate $(drug)_2$:Mg^{2+} complex as the DNA binding ligand in the presence of millimolar concentration of Mg^{2+} [2, 4, 8]. On the other hand, at pH 5.2 neutral CHR forms only the complex with 1:1 stoichiometry even in the presence of millimolar concentration of Mg^{2+} [9, 10]. Spectroscopic studies have shown that the neutral CHR binds to DNA even in the absence of Mg^{2+} with GC-base specificity [9–11]. Spectroscopic characterization of the two Mg^{2+} complexes of CHR, formed at pH 8.0 and the one formed at pH 5.2, followed by a comparison of their DNA binding properties, show that they are different DNA binding ligands [6, 7, 10].

While the above studies partially explain the role of Mg^{2+} in the antibiotic-DNA recognition, so far no model building studies have been carried out with CHR and MTR, to substantiate the above observations. Model building studies associated with the interpretation of NMR spectroscopy of the drug-DNA interaction are also limited to complex II and its binding geometry to oligonucleotides of defined sequences [2, 4, 8]. Therefore, we have undertaken a detailed model building approach to focus on two aspects: Mg^{2+} binding properties of the antibiotic at pH 5.2 and pH 8.0, and its sequence specific association with DNA in presence and absence of Mg^{2+}. Calculations were done only with CHR as experimental studies on DNA binding by neutral MTR is not possible because of its low pK_a. The knowledge from this study would help us in designing tailor made DNA groove binding ligands with GC-base specificity which are rare in the literature.

As it is seen from experimental studies that entropy plays a major role in DNA-CHR interaction, we have carried out Molecular Dynamics (MD) simulations of CHR in different environments and at different protonation states to characterize its relative hydrophobicities in different pH values in the presence and absence of Mg^{2+}. The theoretical trend compares well with experimental results. This property

may be related to aggregation of the free ligands that leads to entropic contribution to the binding free energy during their association with DNA. MD simulation of CHR:Mg^{2+} complex formed at pH 5.2 and complex I also gives an idea about the pH dependent differences in the nature of the 1:1 complex formed between CHR and Mg^{2+}. Finally, simulated annealing followed by energy minimization method has been employed to understand the sequence specific interaction of neutral CHR with DNA in presence and absence of Mg^{2+}. The results have been compared with the scenario when the 1:1 complex of anionic CHR (complex I) interacts with DNA [12]. While calculating theoretical binding free energy, we have taken into account the contributions from structural alterations of DNA and ligand(s) as a sequel to association between them, which has already been shown to play an important role during intercalation of ligand with DNA [13]. Earlier spectroscopic studies for anionic CHR had also suggested such structural changes to be involved during ligand-DNA association [2, 12]. Changes in accessible surface area of the ligand upon association with DNA accounts for the extent of surface complementarity between the ligand and its binding site. Removal of bound water molecules from this interfacial region in the DNA groove and ligand surface gives rise to the entropic contribution to the theoretical free energy of binding [14]. It appears that hydrogen bond plays a less significant role in base specific recognition between ligand and DNA although there are quite a few strong hydrogen bonds between drug and DNA.

2. Methods

We used CHARMM [15] for energy minimization and MD simulation studies with all atom potential, including non-polar hydrogen atoms. We generated the starting coordinates for the ligand using standard bond lengths, bond angles and torsion angles that correspond to stretched out geometry of the large and flexible ligand. Fiber diffraction data [16, 17] provided the coordinates for A- and B- forms of DNA. We generated the coordinates for Mg^{2+} by positioning it equidistant from the OC9 and OC1 atoms (Figure 1) of the antibiotic which are known to be involved in coordinate bond formation with Mg^{2+} in the dimer – Mg^{2+} complex [8].

Bond length, bond angle, dihedral angle energy parameters and van der Waal's parameters for the different bonds and atom of CHR were assigned from the CHARMM parameter file 'par_all22_prot_na.inp' based on similarity with those in the nucleotide or amino acid residues. Some additions were made to the parameter file in order to calculate the energies for the CHR molecule, which were also based on similarity criteria. Partial charges for the atoms of CHR were calculated using GAMESS [18] with HF6-311 G basis set.

We have neutralized negatively charged DNA molecules by adding Na^+ counterions at equal distance (3.23 Å) from the double bonded oxygen atoms of the phosphates. A physical model was used for positioning the ligand in the minor groove of DNA with reasonably well wrapped conformation. We noted the glyc-

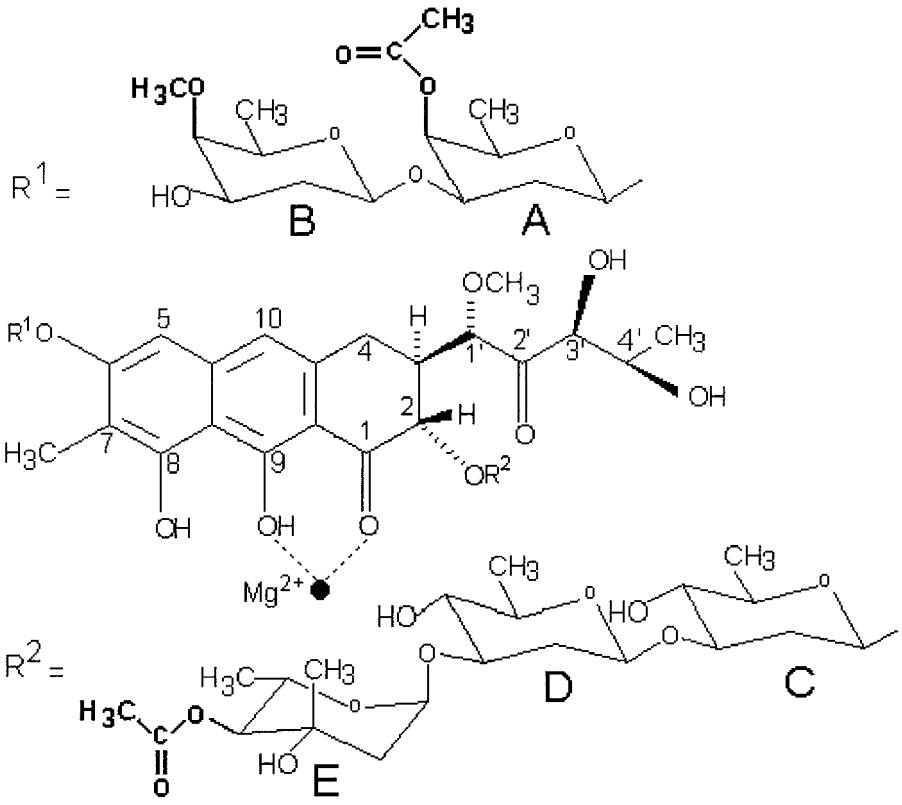

Figure 1. Chemical structure of chromomycin A_3.

osidic torsion angles from the model and employed them to generate the coordinates of the DNA wrapped antibiotic according to published protocol [19]. We solvated all free ligands (CHR, CHR:Mg^{2+} and complex I) and free DNA (including Na^+ counterions) by a 8Å thick layer of TIP3P water molecules [20] having a density of 0.998 g/cm^3, as such a layer effectively mimics completely hydrated systems [21–25]. Such a shell excludes all water molecules within 3Å or farther than 11Å from the central molecule of interest. The DNA-ligand complexes were hydrated with the total number of water molecules used for hydrating the corresponding free ligand and free DNA systems. This made the water shell even thicker in the complexes (about 9Å). Electroneutrality was maintained in every system by introducing necessary number of Cl^- ions. These were introduced by replacing randomely selected buried water molecules from the shell of hydration.

Dodecamers, $(dC\text{-}dG)_6.(dC\text{-}dG)_6$ and $(dG)_{12}.(dC)_{12}$ in both A- and B-DNA conformations were chosen for the study as CHR binds strongly to such GC-sequences [5, 6, 10]. As the antibiotic binds to natural DNA e.g. calf thymus DNA, containing both GC and AT base pairs, we also carried out the study with a mixed sequence, d(AGTACGTGACCT).d(AGGTCACGTACT) with 50% GC con-

tent. The mixed sequence contains small G-C stretches, necessary for the binding of CHR [26]. Studies with the $(dA\text{-}dT)_6.(dA\text{-}dT)_6$ sequences were carried out as control sets, because the antibiotic does not bind with the sequences at either pH. $(dA)_{12}.(dT)_{12}$ sequence was not considered as it does not have the potential to exist in both A- and B-forms of DNA and is characterized by very narrow minor groove where CHR cannot fit in [27, 28].

For ligand-DNA complexes, first we carried out energy minimization with 200 cycles of Steepest Descent followed by Adopted-Basis-Newton-Raphson (ABNR) method till gradient of the root mean square deviation (RMSD) of the coordinates in subsequent iterations was less than 0.1. The minimized structures were then subjected to simulated annealing using the following protocol. They were heated to 400K during a timeperiod of 20 ps. This was followed by cooling to 200K in 50 ps. The structures were then further cooled by energy minimization using 200 steps of SD followed by ABNR till tolerence gradient in RMSD exceeded 0.01. During all calculations we used constant dielectric ($\varepsilon = 1$) value for calculation of electrostatic energies. We truncated the electrostatic and van der Waals interactions at 12Å using a force-switch method to dampen the non-bonded potential between 10Å to 12Å. We have not used Ewald based electrostatic calculation as it has been shown that results from the two methods do not differ significantly for simulations smaller than 1 ns [29]. For molecular dynamics we used the leap-frog verlet method with a 0.001 ps time step for integration. For the free DNA and/or, ligands the structures were minimized using 200 steps of SD followed by ABNR till tolerance gradient in RMSD exceeded 0.01. The final energies of these were compared with the DNA-ligand complexes. Hydrogen bonds were determined using a distance cut off of 2.4Å and angle cut off of 140° [30]. Analysis of DNA conformation was carried out using NUPARM [31]. Solvent Accessible surface area was calculated using CHARMM with a probe radius of 1.6Å.

Properties of the free ligands were characterized from a separate set of molecular dynamics simulation study. Here, the solvated ligands were first energy minimized with 2000 steps of SD followed by ABNR till tolerence gradient of RMSD exceeded 0.1. These were then heated to 300K within 20 ps. We assigned the velocities using gaussian distribution function. We then equilibrated the system at 300K for 450 ps where we reassigned velocities whenever temperature deviated from target 300K by more than 10°. The production runs were N.V.E. simulations of the systems for 550 ps without any further velocity reassignment. At this stage of simulation, the coordinates were saved after every 0.1 ps interval for further analysis. Final analysis showed that hydration shell is stable with evaporation of one or two water molecules only.

3. Results and Discussion

Computer simulation of Chromomycin A_3 in the absence of DNA: Energy minimization followed by extensive molecular dynamic simulation were carried out

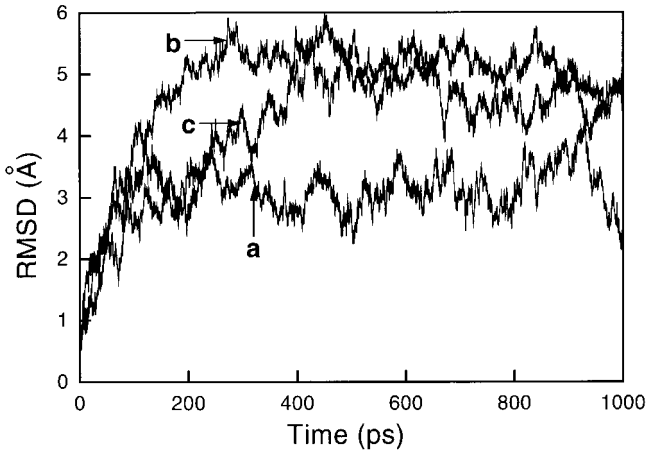

Figure 2. Root mean square deviation of coordinates (Å) for CHR during MD simulation: neutral CHR at pH 5.2 (a); CHR:Mg^{2+} complex at pH 5.2 (b); complex I at pH 8.0 (c).

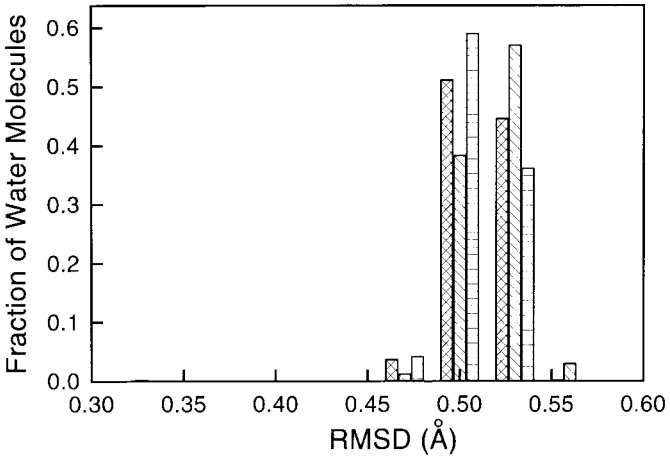

Figure 3. Frequency histograms representing RMS deviation (Å) in the coordinates of water molecules from their preceding position which effectively measures speed of these molecules: Neutral CHR at pH 5.2 (▩); CHR:Mg^{2+} complex at pH 5.2 (▧); Complex I at pH 8.0 (▤); RMS deviations are mean over 550 ps simulation time.

for the three free ligands, neutral CHR, CHR:Mg^{2+} complex formed by neutral drug and complex I formed by negatively charged CHR. Root mean square (RMS) deviations of CHR moiety in the three ligands (Figure 2) indicate that the systems stabilized after 450 ps. The last 550 ps was used for analysis.

An attempt was made to theoretically characterize the hydrophobic properties of the free ligands. Although it is generally believed that a hydrophobic molecule creates a clathrate like water structure around itself [32], recent simulation studies indicate existence of mobile water in the hydration shell of a hydrophobic molecule

[33]. The dynamic nature of the water molecules surrounding the ligand can be assessed from the principal axes momenta (PAX) values for individual atoms of water molecules in the hydration shell of the three systems. Generally much larger values of PAX are obtained for the water molecules around CHR:Mg^{2+} complex, in comparison with that of CHR alone. The PAX values are extremely small for the water molecules around complex I. Since high mobility of the solvent molecules denote absence of bound water in the hydration shell of the central molecule, the above results imply that the CHR:Mg^{2+} complex has the minimum surface hydrophilicity, or the highest hydrophobicity amongst the three systems. This is closely followed by neutral CHR in the absence of a metal ion whereas complex I is found to be highly hydrophilic. The RMS deviations in the position of each water molecule with respect to its preceding position (0.1 ps time interval) is equivalent to average mobility of water molecule including its rotational movement. The values were calculated after each 0.1 ps step, by superposing the ligand to its previous position, and then determining RMS deviation for the individual water molecules. The RMS deviations thus reflect only the relative mobility of water with respect to the central molecule. RMS deviations over a total period of 550 ps for the water molecules were compared between the three systems. In the case of CHR:Mg^{2+} complex a greatest fraction of water molecules show high mean RMS. It is slightly lower for neutral CHR alone and still lower for complex I. Figure 3 illustrates the mean RMS deviations for the water molecules in each system. The distribution shown in Figure 3 also indicates highest hydrophobicity for CHR:Mg^{2+} having highly mobile hydration shell. This is followed by neutral CHR and complex I which even has three water molecules coordinating with the Mg^{2+} ion. The trend in mobilities is similar with that obtained from comparison of their PAX values.

High hydrophobicity in case of CHR:Mg^{2+} and free neutral CHR leads to intermolecular association of the molecules in an entropy driven fashion. Such association is also indicated from the highest value of fluorescence polarization anisotropy (FPA) [34] of CHR:Mg^{2+} complex among the three species. The trend of FPA values for the other two species is also commensurate with the extent of intermolecular hydrophobic association. FPA values follow the order, CHR:Mg^{2+}, 0.260 $>$ Neutral CHR, 0.095 $>$ Complex I, 0.024 [10]. Complex I is the least hydrophobic species and, therefore, does not undergo any aggregate formation.

Analysis of Chromomycin A_3-DNA Interaction: We employed simulated annealing followed by energy minimization to study CHR-DNA interaction in order to obtain their complex in the most stable conformation. Heating the ligand-DNA complex(es) during simulated annealing facilitates the molecules to search for their energetically favored geometry away from local minimum near the starting conformation. Above studies were focussed to assess (i) binding potential of neutral CHR and its Mg^{2+} complex and (ii) the origin of GC base specificity exhibited by these ligands.

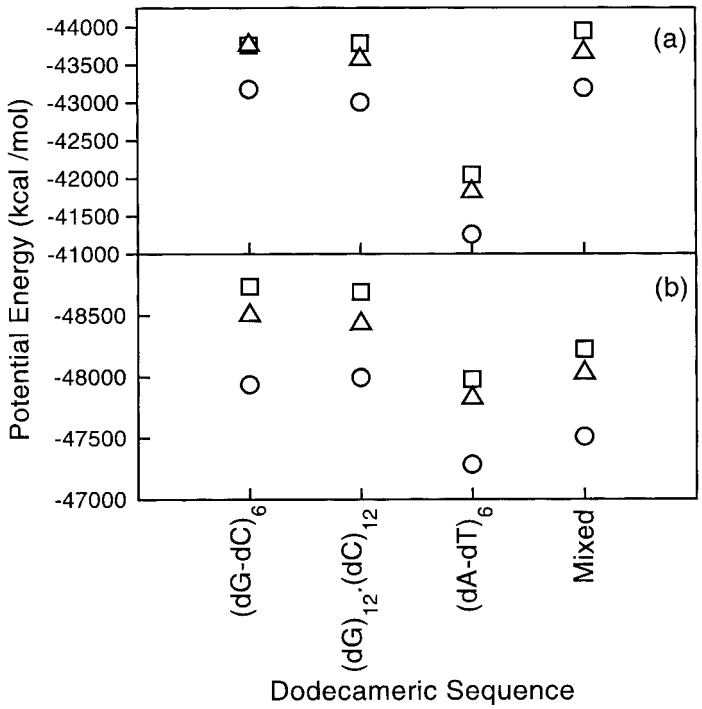

Figure 4. Potential energy of ligand-DNA complexes for different dodecameric sequences in (a) A-form and (b) B-form. Neutral CHR (○); CHR:Mg^{2+} complex at pH 5.2 (□); Complex I (△).

Results from above studies indicate that both neutral CHR and its Mg^{2+} complex have the potential for binding to DNA. This is concluded from high negative potential energy values obtained for the above systems (Figure 4). The energy values are comparable to those obtained for the interaction(s) of complex I, with the different DNA sequences. Since complex I of CHR is a known DNA binding ligand [6], the binding potential of neutral CHR and its Mg^{2+} complex could be concluded from the above comparison. However, reasonably high negative energy values were also obtained for fully AT containing sequences thereby indicating that total potential energy does not indicate the base sequence specific nature of CHR-DNA association. Since it includes major contribution from stabilization energy of the base-paired DNA molecule and additional contribution from DNA-ligand interaction energy, high values are obtained even for the AT containing sequences. Thus all dodecameric sequences give reasonably good values for total potential energy.

In order to understand the base sequence specific interaction, we evaluated the direct interaction energies between the ligand(s) and DNA for different sequences from the coordinates of the minimized CHR-DNA complexes (Table I). They show that the binding is several folds stronger for CHR:Mg^{2+} complex and complex I

Table I. Interaction energy for association of chromomycin A_3 with dodecanucleotides in absence and presence of Mg^{2+}

Sequence	Ligand	B-DNA		A-DNA	
		Net Interaction Energy (kcal/mol)[a]	Direct Interaction Energy (kcal/mol)	Net Interaction Energy (kcal/mol)[a]	Direct Interaction Energy (kcal/mol)
$(dG)_{12}(dC)_{12}$	CHR	–3353.1	–83.9	–1653.5	–86.8
$(dG\text{-}dC)_6$	CHR	–3294.0	–66.4	–1678.8	–107.21
$(dA\text{-}dT)_6$	CHR	–3105.3	–83.9	–1577.6	–74.0
Mixed	CHR	–3288.1	–56.3	–1636.2	–102.6
$(dG)_{12}(dC)_{12}$	CHR:Mg^{2+}	–3423.8	–348.9	–1678.6	–154.0
$(dG\text{-}dC)_6$	CHR:Mg^{2+}	–3261.5	–497.0	–1730.7	–494.4
$(dA\text{-}dT)_6$	CHR:Mg^{2+}	–3074.6	–490.2	–1642.9	–382.5
Mixed	CHR:Mg^{2+}	–3273.8	–360.5	–1663.8	–461.7
$(dG)_{12}(dC)_{12}$	Complex I	–3361.9	–268.4	–1683.0	–385.0
$(dG\text{-}dC)_6$	Complex I	–3175.4	–286.9	–1690.0	–429.0
$(dA\text{-}dT)_6$	Complex I	–3090.5	–434.7	–1583.5	–430.0
Mixed	Complex I	–3250.5	–268.6	–1547.5	–327.0

[a] Net Interaction Energy = Potential Energy of ligand-DNA complex- [Potential Energy of free DNA + Potential Energy of free ligand].

as compared to the free neutral antibiotic. However the trend in these values is not commensurate with the experimental binding specificity. This is because of a major limitation in the direct interaction energy approach. It only considers the interaction between the ligand and DNA in their bound form and ignores contributions arising from (i) deformation(s) in ligand and DNA geometry upon complex formation and (ii) changes in hydration and/or counterion disposition around the DNA and ligand. Experimental results from ours and other groups [2, 10, 12] indicate that proper interpretation of binding necessitates the consideration of structural distortions of both the ligand and DNA. The net enthalpy change associated with the ligand-DNA interaction could thus be expressed as a sum of two contributions. Favorable enthalpy change arises from binding of ligand to DNA, while another term due to conformational enthalpy change of DNA at the ligand binding site and that of the ligand also has to be considered. In most cases the second term contributes unfavorably to total enthalpy. Figure 5 illustrates a representative example for structural alterations in DNA upon complex formation in terms of local dinucleotide step parameter, roll. It shows that such distortions cannot be ignored and the same is true for the ligands also (data not shown). Thus, theoretical interaction energy values which are comparable to the enthalpy change values for the association process should also include such distortion energy terms. This was achieved by determining

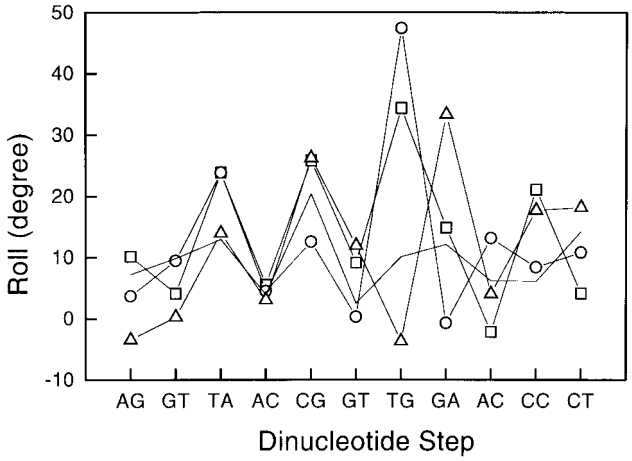

Figure 5. Roll angle for d(AGTACGTGACCT).d(AGGTCACGTACT) in the absence and presence of different ligands. Free DNA (——); Neutral CHR (– ○ –); CHR:Mg^{2+} complex at pH 5.2 (– □ –); Complex I (– △ –).

the net interaction energy. This is calculated by subtracting the potential energies of the free minimized ligand and minimized unliganded DNA from the total potential energies of the ligand-DNA complexes. This takes into account the changes in energy due to conformational change of the DNA and the unbound ligand during complex formation and change in energy due to alteration in hydration at their interaction surface. A similar approach was adopted by Kollman and co-workers during their study of sequence specific drug-DNA interaction in absence of counterions and water [13]. The trend in the net energy values for different sequences matches well with the experimentally observed GC-base specificity of the ligand.

Net interaction energy values thus explain experimental base specificity of the antibiotic on the basis of enthalpic contribution to the free energy change associated with the interaction. Additional entropy term would cumulatively determine binding potentials of the ligands with different DNA sequences. In order to get a quantitative picture about entropy changes during complex formation we examined the changes in accessible surface area of the ligand associated with the ligand-DNA interactions (Table II). Analysis of these values show that during interaction of CHR with DNA in the presence of Mg^{2+}, a relatively larger surface area gets buried. This implies an enhanced degree of penetration by the ligand into the minor groove leading to a entropy gain through release of solvent molecules. Such changes in accessible surface area are consistently lower in the absence of the metal ion. This indicates that entropy change plays a major role during association of CHR:Mg^{2+} complex with DNA in comparison to free neutral CHR. Similar changes in the accessible surface area for the association of complex I with DNA, which binds to DNA in entropy driven fashion [10], further implies that the chromomycinone moiety of the ligand undergoes enhanced degree of penetration

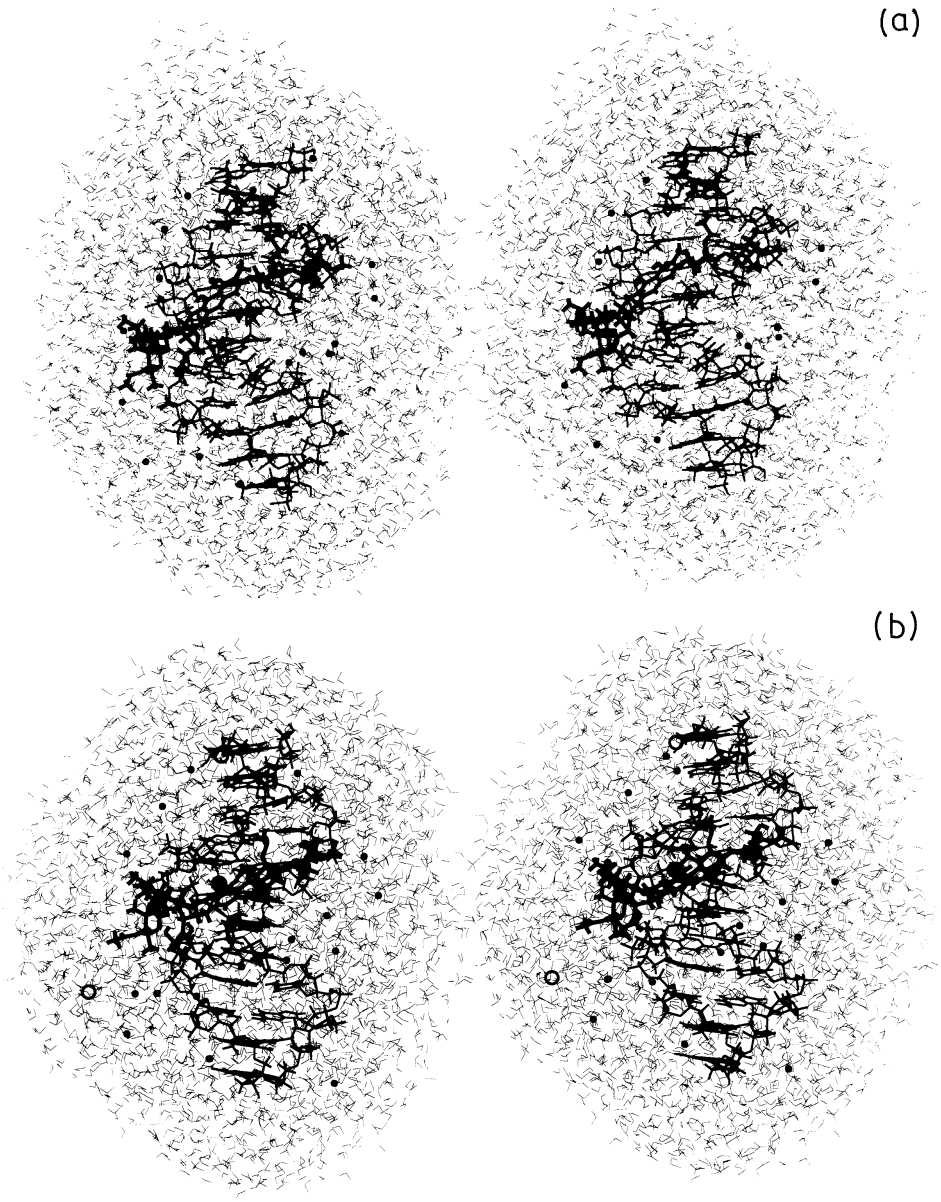

Figure 6. Stereo diagrams of the structures of the ligand bound dodecamers for some representative sequences after final energy minimization. (a) neutral CHR bound to B-DNA sequence d(AGTACGTGACCT).d(AGGTCACGTACT); (b) CHR:Mg^{2+} complex bound to B-DNA sequence $(dC\text{-}dG)_6.(dC\text{-}dG)_6$; (c) complex I bound to A-DNA sequence $(dG)_{12}.(dC)_{12}$. Water molecules in the shell of hydration are drawn with very thin lines. DNA molecule is drawn with line of intermediate thickness and ligand with thick line. Large filled circle represents the Mg^{2+} ion; Na^{+} ions are shown as small filled circle. In systems containing Cl^{-} ion, it is shown as large empty circle.

Table II. Changes in accessible surface area of ligand and DNA upon complex formation

Sequence	DNA Form	ΔSurface[a] for CHR-DNA complex (Å^2)	ΔSurface[a] for CHR:Mg^{2+}-DNA complex (Å^2)	ΔSurface[a] for complex I-DNA complex (Å^2)
$(dG)_{12}(dC)_{12}$	B	–998	–1190	–1039
$(dG\text{-}dC)_6$	B	–1001	–1130	–1065
$(dA\text{-}dT)_6$	B	–956	–1351	–1281
Mixed	B	–1131	–1153	–1193
$(dG)_{12}(dC)_{12}$	A	–1202	–1342	–1330
$(dG\text{-}dC)_6$	A	–1176	–1468	–1277
$(dA\text{-}dT)_6$	A	–1069	–983	–881
Mixed	A	–1650	–1558	–1233

[a] ΔSurface = Accessible surface area of ligand-DNA complex-[accessible surface area of free DNA + accessible surface area of free ligand].
Surface area of free CHR, CHR:Mg^{2+} and complex I are 1660 Å^2, 1704 Å^2 and 1698 Å^2, respectively.

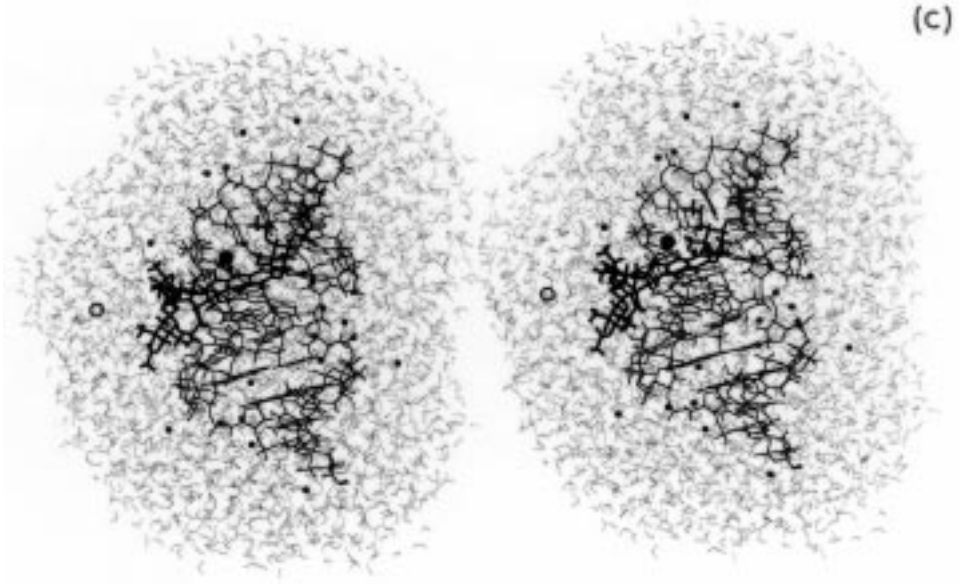

Figure 6. Continued.

Table III. Hydrogen bonds formed between ligand and DNA upon complex formation

Sequence	DNA	CHR-DNA complex		CHR:Mg^{2+}-DNA complex		Complex I-DNA complex	
		H-Bonds (Å)	Donor-Acceptor[a]	H-Bonds (Å)	Donor-Acceptor[a]	H-Bonds (Å)	Donor-Acceptor[a]
$(dG)_{12}(dC)_{12}$	B	2.1	2-NH_2(G19)-CHR(E)	–	–	–	–
		1.9	CHR(E)-O4′(C7)				
$(dG\text{-}dC)_6$	B	–	–	2.1	CHR(E)-O1 P(C8)	1.8	CHR(E)-O1 P(C8)
$(dA\text{-}dT)_6$	B	–	–	2.1	CHR(aur)-O2(T10)	1.7	CHR(aur)-O1 P(T20)
				2.0	CHR(E)-O3′(A7)		
Mixed	B	–	–	2.2	CHR(E)-O3′(T7)	1.9	CHR(E)-O3′(T7)
$(dG)_{12}(dC)_{12}$	A	2.0	2-NH_2(G16)-CHR(aur)	1.8	Nh_2(G7)-CHR(C)	1.8	2-NH_2(G16)-CHR(aur)
		2.3	2-NH_2(G17)-CHR(aur)			2.0	2-NH_2(G19)-CHR(E)
$(dG\text{-}dC)_6$	A	1.9	2-NH_2(G9)-CHR(aur)	2.3	NH_2(G7)-CHR(E)	2.0	2-NH_2(G7)-CHR(C)
		1.9	2-NH_2(G17)-CHR(aur)	2.3	NH_2(G9)-CHR(A)	2.1	2-NH_2(G19)-CHR(E)
		2.1	2-NH_2(G19)-CHR(E)				
		1.8	CHR(aur)-O3′(C18)				
$(dA\text{-}dT)_6$	A	2.2	CHR(aur)-O2(T10)	2.3	CHR(aur)-N3(A9)	–	–
Mixed	A	–	–	2.4	NH_2(G8)-CHR(aur)	–	–

[a] Atoms of CHR involved in H-bonding are marked by the sugar or aureolic acid moiety to which it belongs. DNA atoms forming H-bond are explicitly named and corresponding base is numbered.

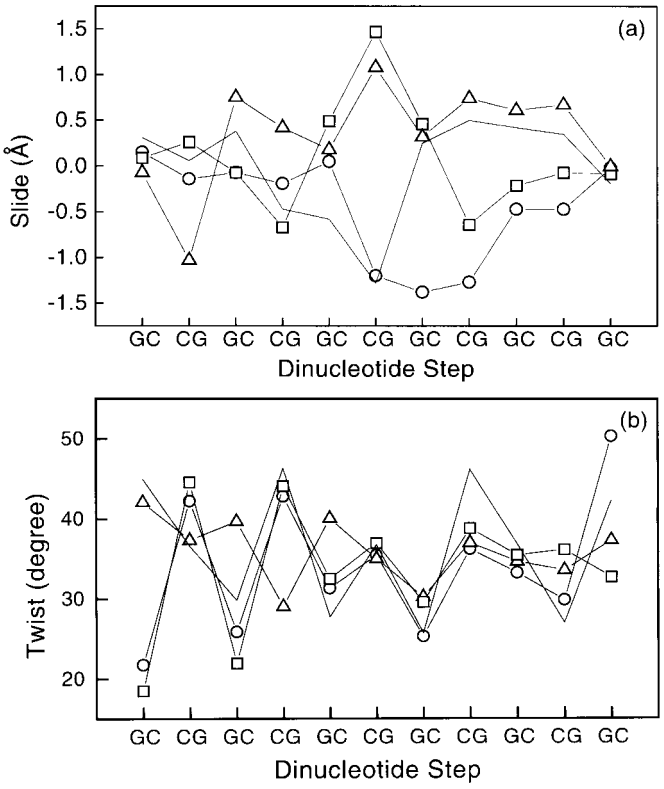

Figure 7. Dinucleotide step parameters for $(dG\text{-}dC)_6$ in the absence and presence of different ligands. (a) Slide (b) Twist angle. In each case the following symbols have been used: Free DNA (——); Neutral CHR (– ○ –); CHR:Mg^{2+} complex at pH 5.2 (– □ –); Complex I (– △ –).

only in the presence of the metal ion. The role of metal ion during association of the ligand with DNA is thus similar for neutral and anionic CHR.

Figure 6 depicts the binding geometries of CHR, CHR:Mg^{2+} complex and complex I with representative DNA sequences. In general, CHR stays at the periphery of the B-DNA minor groove when it complexes with DNA in the absence of Mg^{2+}. On the other hand, the aureolic acid chromophore of CHR:Mg^{2+} complex and complex I penetrates into the minor groove. This is indicated in Figure 7a which illustrates the relative displacement of base pairs, slide, for a B-DNA sequence $[(dG\text{-}dC)_6]$ following complexation with the three ligands. The values are found to be considerably more positive for the Mg^{2+} containing ligands, where the basepairs are pushed towards the major groove. For the same sequence however other conformational parameters remain unaffected (twist values are shown in Figure 7(b) as an example). In case of A-DNA, all ligands bind close to the base pairs in the shallow and wider minor groove. This leads to a difference in the binding geometry of the same ligand with A- and B-DNA. Differences in the extent of groove access-

ibility by the ligands in the presence and absence of Mg^{2+}, for B-DNA sequences is also apparent from the accessible surface area calculations.

Since NMR studies by different groups [2, 4, 8] have earlier indicated the importance of H-bonding with DNA bases during GC-base specific interaction of complex II of CHR with DNA, we also examined the possibility of H-bond formation from the optimized coordinates of the ligand-DNA complexes. Hydrogen bonds were detected using a cutoff distance of 2.4Å between hydrogen and the acceptor atom. Such long distance hydrogen bonds are mostly observed in drug-DNA crystal structures [30]. We observed that for B-DNA sequences there are lesser number of H-bonds formed between the antibiotic and DNA bases for all the three ligands. On the other hand there are large number of H-bonds formed with the A-form of DNA (Table III). It is seen that apart from H-bonding between aureolic acid group and DNA bases as proposed by NMR studies, there are several H-bonds between the E-sugar of the ligands (which has additional acetoxy group) with DNA bases, phosphates and sugar moieties. This possibly explains differential binding nature of the two very similar ligands, CHR and MTR [12]. Therefore our results did not give conclusive evidence regarding the role of H-bonds in determining the base specificity by neutral CHR, CHR:Mg^{2+} complex and complex I. It is however, not surprising, since specific H-bond formation is not the major driving force for the association of many sequence specific minor groove binding ligands, both proteins and antibiotics [30, 35, 36]. For these molecules, the important parameters for specific recognition are the curvature and dimension of the minor groove at the ligand binding site, which are indeed base sequence dependent [28].

The results from the model building studies for the neutral and anionic antibiotic show that CHR molecule has the structural potential to bind to DNA even in the absence of metal ion and it establishes models for CHR-DNA and CHR:Mg^{2+}-DNA interactions at pH 5.2. With the knowledge from the present study, we plan to understand in greater detail the association of the two ligands, complexes, I and II, with DNA at and above physiological pH. Work in this area is currently underway in our laboratory.

Acknowledgement

S.C. wishes to thank Prof Dr B.K. Sinha, Director of S.I.N.P. for his kind permission to allow her to work in the Biophysics Division of the Institute.

References

1. Chabne, B.A., Allegra, C.J., Curt, G.A. and Calabresi, P.: The Pharmacological Basis of Therapeutics, 9th edition, In: J.G. Hardman, L.E. Limbird, P.B. Molinoff, R.W. Ruddon and A.G. Gilman (eds.), McGraw-Hill, New York, 1996.
2. Gao, X. and Patel, D.J.: *Biochemistry* **28** (1989), 751–762.
3. Bailly, C., and Waring, M.J.: *Nucleic Acids Res.* **23** (1995), 885–892.

4. Keniry, M.A., Banville, D.L., Simmonds, P.M. and Shafer, R.: *J. Mol. Biol.* **231** (1993), 753–767.
5. Nayak, R., Sirsi, M. and Podder, S.K.: *FEBS Lett.* **30** (1973), 157–162.
6. Aich, P., Sen, R. and Dasgupta, D.: *Biochemistry* **31** (1992), 2988–2997.
7. Aich, P., Sen, R. and Dasgupta, D.: *Chem. Biol. Interact.* **83** (1992), 23–33.
8. Sastry, M. and Patel, D.J.: *Biochemistry* **32** (1993), 6588–6604.
9. Aich, P.: Ph.D Thesis entitled *Molecular Basis of Interaction of the Antitumor Antibiotics, Mithramycin and Chromomycin A_3, with Deoxyribonucleic Acid*, Jadavpur University (1993).
10. Chakrabarti, S., Aich, P., Sarker, D., Bhattacharyya, D. and Dasgupta, D.: *J. Biomol. Struct. Dynam.* **18** (2000), 209–218.
11. Weinberger, S., Shafer, R. and Berman, E., *Bioploymers* **27** (1988), 831–842.
12. Majee, S., Sen, R., Guha, S., Bhattacharyya, D. and Dasgupta, D.: *Biochemistry* **36** (1997), 2291–2299.
13. Lybrand, T.P., Brown, S.C., Creighton, S., Shafer, R.H. and Kollman, P.A.: *J. Mol. Biol.* **191** (1986), 495–507.
14. Novotny, J., Bruccoleri, R.E. and Saul, F.A.: *Biochemistry* **28** (1989), 4753–4749.
15. Brooks, B.R., Bruccoleri, R.E., Olafson, B.D., States, D.J., Swaminathan, S. and Karplus, M.: *J. Comp. Chem.* **4** (1983), 187–217.
16. Chandrasekaran, R. and Arnott, S.: *J. Biomol. Struct. Dynam.* **13** (1996), 1015–1027.
17. Chandrasekaran, R., Wang, M., He, R.G., Puigjanar, L.C., Byler, M.A., Millane, R.P. and Arnott, S.: *J. Biomol. Struct. Dynam.* **6** (1989), 1189.
18. Schmidt, M.W., Baldridge, K.K., Boatz, J.A., Elbert, S.T., Gordon, M.S., Jensen, J.H., Koseki, S., Matsunaga, N., Nguyen, K.A., Su, S., Theresa, L.W., Dupuis, M., Montogomery, J.A. Jr.: *J. Comp. Chem.* **14** (1993), 1347–1363.
19. Gopalkrishnan, B. and Bansal, M.: *J. Biomol. Struct. Dynam.* **5** (1988), 859–871.
20. Jorgenson, W.L., Chandrasekhar, J., Medura, J.D., Impey, R.W. and Klein, M.L.: *J. Chem. Phys.* **79** (1983) 926–935.
21. Steinbach, P.J. and Brooks, B.R.: *Proc. Natl. Acad. Sci. USA.* **90** (1993), 9135–9139.
22. Bhattacharyya, D., Brooks, B.R. and Callahan, L.: *Aids Research and Human Retroviruses* **12** (1996), 83–90.
23. Elofsson, A. and Nilsson, L.: *J. Mol. Biol.* **233** (1993) 766–780.
24. Arnold, G.E. and Ornstein, R.L.: *Proteins* **18** (1994), 19–33.
25. Sen, S. and Nilsson, L.: *Biophys J.* **77** (1999), 1782–1800.
26. Fox, K.R. and Howarth, N.R.: *Nucleic Acids. Res.* **13** (1985), 8695–8713.
27. Saenger, W.: *Principles of Nucleic Acid Structure*, Springer-Verlag New York Inc, 175 Fifth Avenue, New York, U.S.A, 1984.
28. Calladine, C.R. and Drew, H.R.: *Understanding DNA-The Molecule & How It Works*, Academic Press Inc., 24–28 Oval Road, London, U.K, 1992.
29. Darden, T., Perera, L., Leping, L. and Pedersen, L.: *Structure* (1999), 7, R55.
30. Tabernero, L., Bella, J. and Aleman, C.: *Nucleic. Acids Res.* **24** (1996), 3458–3466.
31. Bansal, M., Bhattacharyya, D. and Ravi, B.: *Comput. Appl. Biosci.* **11** (1995), 281–287.
32. Kauzmann: *Adv. Prot. Chem.* **14** (1959), 1–63.
33. Fidler, J. and Rodger, P.M.: *J. Phys. Chem.* **B103** (1999), 7695–7703.
34. Lakowicz, J.R.: *Principles of Fluorescence Spectroscopy*, Plenum Press, New York, 1983.
35. Werner, M.H., Gronenberg, A.M. and Clore, G.M.: *Science* **271** (1996), 778–784.
36. von Hippel, P.H.: *Science* **263** (1994), 769–770.